Novel Biobased Nanocomposites from Soybean Oil and Functionalized Organoclay

Yongshang Lu and Richard C. Larock*

Department of Chemistry, Iowa State University, Ames, Iowa 50011, USA

Received May 11, 2006; Revised Manuscript Received July 17, 2006

Novel biobased nanocomposites have been prepared by the cationic polymerization of conjugated soybean oil (CSOY) or conjugated LoSatSoy oil (CLS) with styrene (ST) and divinylbenzene (DVB), and a reactive organomodified montmorillonite (VMMT) clay as a reinforcing phase. This filler has been prepared by the cationic exchange of sodium montmorillonite with (4-vinylbenzyl)triethylammonium chloride in aqueous solution. The nanostructures of the nanocomposites have been determined by using wide-angle X-ray diffraction (WAXD) and transmission electron microscopy (TEM), respectively. The results from WAXD and TEM indicate that a heterogeneous structure consisting of intercalation and partial exfoliation or an intercalation structure exists in the nanocomposites, depending on the amount of VMMT in the polymer matrix. The thermal, mechanical, and organic vapor barrier properties of the nanocomposites have been evaluated by dynamic thermal analysis, thermogravimetric analysis, mechanical testing, and toluene absorption. A significant improvement is observed in the thermal stability, the dynamic bending storage modulus, the compressive modulus, the compressive strength, the compressive strain at failure, and the vapor barrier performance for the CSOY- and CLS-based nanocomposites with 1−2 wt % VMMT loading, where some individual exfoliated silicate platelets occur. For example, the CLS-based nanocomposite with 1−2 wt % VMMT exhibits increases of 100−128%, 86−92%, and 5−7% in compressive modulus, compressive strength, and compressive strain at failure, respectively. CLS with higher unsaturation and reactivity affords nanocomposites with higher thermal stability and higher mechanical properties than CSOY.

Introduction

Polymer−clay nanocomposites have attracted increasing attention from science and industry.[1] Compared with conventional composites with higher filler concentrations, nanocomposites often exhibit a great improvement in modulus,[2−5] creep resistance,[6] strength,[7,8] heat resistance,[9] and barrier[10−12] and fire-retardant properties[13−15] at very low clay contents of generally less than 5 wt %. The main reason for these improved properties in the polymer−clay nanocomposites is the strong interfacial interactions between the matrix and the layered silicate as opposed to conventional composites.[16] Montmorillonite (MMT), by far the most commonly used clay for the preparation of polymer−clay nanocomposites, is a crystalline 2:1 layered clay mineral with a central alumina octahedral sheet sandwiched between two silica tetrahedral sheets.[17] When these high aspect ratio (e.g. 10−1000) nanoparticles are dispersed into a polymer, they can be either intercalated by the polymer chains or individually exfoliated within the polymer matrix to form nanocomposites.[17,18] Many polymer/clay nanocomposites have been successfully developed by inserting the polymer chains into the silicate galleries.[19] The intercalation of polymer chains into the silicate galleries is generally done by using one of the following methods: insertion of suitable monomers into the silicate galleries and subsequent polymerization[20−24] or directly inserting polymer chains into the galleries from either a solution or a melt.[25−28] However, the hydrophilic characteristic of MMT makes it difficult for hydrophobic polymer chains to intercalate into the layered silicate galleries. Thus, it is usually necessary to modify the inorganic MMT by substituting the cations in the MMT galleries with quaternary alkylammonium salts, which can significantly improve the compatibility between MMT and the polymers, and thus optimize the performance of the resulting materials.[29]

For sustainable development, the use of renewable resources has attracted the attention of many researchers because of their potential substitution for petrochemical derivatives.[30] The petroleum shortage has stimulated research on alternative and renewable materials for the preparation of polymers from plant products, especially from renewable resource plant oils.[31] Lately, considerable research has been concentrated on the development of biobased polymers using natural oils or their derivatives as the main comonomer. Promising results have been reported on copolymer resins from acrylated epoxidized soybean oil and styrene (ST),[32,33] epoxy resins based on epoxidized soybean or linseed oils,[34] and polyurethane thermosets[35] and aqueous dispersions[36,37] from soybean, rapeseed, and castor oils. In our previous work, we have taken advantage of the carbon−carbon double bonds in soybean,[38−41] linseed,[42] tung,[43,44] corn,[45] and fish oils[46] to develop a wide variety of new polymeric materials by the cationic or thermal copolymerization of these natural oils with ST and divinylbenzene (DVB) or dicyclopentadiene. The resulting thermosetting polymers can be varied from elastomers to tough and rigid plastics by simply changing the stoichiometry, the type of oil, and the alkene comonomers. These new polymers exhibit thermophysical and mechanical properties that are comparable to those of commercially available elastomers and conventional plastics and may serve as replacements for petroleum-based polymers in many applications.[47]

Recently, Wool et al.[48] have prepared biobased nanocomposites by dispersing an organoclay in acrylated epoxidized soybean oil and ST, followed by free radical polymerization.

* To whom all correspondence should be addressed. Phone: +1-5152944660. Fax: +1-5152940105. E-mail: larock@iastate.edu

10.1021/bm060458e CCC: $33.50
Published on Web 08/23/2006

Kobayashi et al.[49,50] and Mohanty et al.[51] have developed nanocomposites by acid-catalyzed curing and anhydride curing of epoxidized linseed and soybean oils, respectively, in the presence of an organoclay. The resulting nanocomposites show improved mechanical properties,[48−51] thermal stability,[48−51] and barrier properties,[49] when compared to the pure polymer alone. Soybean oil (SOY) and LoSatSoy oil (LSS) consist of triglyceride molecules with respectively, on average, approximately 4.5 and 5.1 C═C bonds per molecule in the fatty-acid side chains, which makes it possible to copolymerize SOY and LSS directly with other comonomers by cationic polymerization.[38−40] The conjugated soybean oil (CSOY) and the conjugated LoSatSoy oil (CLS) have the same degree of unsaturation as the SOY and LSS, but essentially all of the carbon−carbon double bonds that can be conjugated in the SOY and LSS are conjugated in the CSOY and CLS, respectively, which imparts a higher reactivity to the CSOY and CLS than the SOY and LSS, which in turn results in polymers with much improved properties.[38] So we, in this study, have explored the feasibility of cationic polymerization of CSOY and CLS with ST and DVB in the presence of an organoclay to prepare the novel nanocomposites. The organclay used in this work was modified with (4-vinylbenzyl)triethylammonium chloride (VTAC), so that the organoclay can be polymerized into the polymer matrix by chemical bonding during polymerization, leading to a significant performance improvement for the resulting nanocomposites when compared with the corresponding pure polymers. The morphology, structure, thermal stability, and mechanical and barrier properties of the resulting nanocomposites have been carefully investigated by wide-angle X-ray diffraction (WAXD), transmission electronic microscopy (TEM), dynamic mechanical analysis (DMA), thermogravimetric analysis (TGA), mechanical testing, and toluene absorption.

Experimental Section

Materials. Wesson soybean oil (SOY) and LoSatSoy oil (LSS, Zeeland Food Service Inc. MI) were purchased at the local supermarket and used directly without further purification. The conjugated soybean oil (CSOY) and conjugated LoSatSoy oil (CLS) were synthesized by the rhodium-catalyzed isomerization of SOY and LSS using a method developed previously by us.[52] The degree of conjugation was calculated to be about 100% as determined by ^{1}H NMR spectroscopy on a Varian Unity spectrometer (Varian Associates, Palo Alto, CA) at 300 MHz. Na−montmorillonite (MMT) powder with a cation exchange capacity of 76.4 mequiv/100 g was obtained from Source Clay Minerals Repository Co. under the trade name Swy-2. Styrene (ST), divinylbenzene (DVB) (80 mol % divinylbenzene and 20 mol % ethylvinylbenzene), 4-vinylbenzyl chloride, triethylamine, and distilled-grade boron trifluoride diethyl etherate (BFE) were purchased from Aldrich Chemical Co. and used as received. Norway Pronova fish oil ethyl ester EPAX 5500 EE (NFO) was used to modify the cationic initiator.

Functionalization of MMT. (4-Vinylbenzyl)triethylammonium chloride (VTAC) was prepared by the reaction of 4-vinylbenzyl chloride with triethylamine (1.3 equiv) in diethyl ether at ambient temperature for 72 h. The precipitate was filtered, washed with diethyl ether, and dried under vacuum to obtain a white powder of VTAC.

The MMT was ground and screened with a 325 mesh sieve. To a 500 g aqueous dispersion of 2 wt % MMT (0.00764 mol Na^+), 2.32 g of VBAC (0.00917 mol) was added gradually under stirring at 80 °C. After 4 h, the exchanged clay was filtered and washed with distilled water until no chloride ion was detected with a 0.1 M $AgNO_3$ solution. The VTAC-functionalized MMT (VMMT) was dried in a vacuum oven at room temperature and then used for the synthesis of nanocomposites.

Synthesis of CSOY- and CLS-Based Nanocomposites. The desired amount of VMMT was dispersed into the mixture consisting of 50 g of CSOY (or CLS), 25 g of ST and 10 g of DVB. The resulting mixture was vigorously stirred for 24 h, followed by sonication for 4 h at room temperature. Then, 15 g of the modified BFE initiator, prepared by mixing the NFO with BFE in a 2:1 weight ratio, was added. The NFO is added for production of more homogeneous reactions and polymers. The resulting reactants were cured for 2 h at room temperature, followed by 2 h at 60 °C, 2 h at 80 °C, and 12 h at 110 °C. By changing the VMMT loading of 0, 1, 2, 3, and 5 wt %, a series of nanocomposites from CSOY and CLS were prepared in which the VMMT is expressed as a percent of the total weight. The nomenclature used for the soybean oil-based polymer matrix is the following: CSOY, CLS and NFO represent conjugated soybean oil, conjugated LoSatSoy oil and Norway Pronova fish oil ethyl ester, respectively; ST and DVB are the styrene and divinylbenzene comonomers; and BFE is the boron trifluoride diethyl etherate initiator. For example, CSOY50−ST25−DVB10−NFO10−BFE5 corresponds to a polymer matrix prepared from 50 wt % CSOY, 25 wt % ST, 10 wt % DVB, 10 wt % NFO, and 5 wt % BFE initiator.

Characterization. Wide angle X-ray diffraction (WAXD) analysis was performed at room temperature using a Scintag XDS-2000 diffractometer with Cu $_{K\alpha}$ ($\lambda = 0.154$ nm) radiation at 40 kV and 30 mA. The diffractograms were scanned from 2 to 10° at a rate of 1°/min. The morphology of the nanocomposites was examined on a transmission electron microscope (JEOL 1200EX) using an acceleration voltage of 120 kV. Samples were cut into 60−80 nm thick sections with a diamond knife at −100 °C.

The dynamic mechanical properties of the nanocomposites were obtained with a Perkin-Elmer dynamic mechanical analyzer (Pyris-7e) (Perkin-Elmer, Norwalk, CT) in a three-point bending mode at a frequency of 1 Hz under helium and a heating rate of 5 °C/min. Rectangular specimens of about 2 mm × 5 mm × 10 mm were used.

A Perkin-Elmer Pyris-7 thermogravimeter was used to measure the weight loss of the nanocomposites under an air atmosphere. The samples were heated from 100 to 650 °C at a heating rate of 20 °C/min. Generally, 10−15 mg samples were used for the thermogravimetric analysis.

The compressive mechanical tests have been performed according to ASTM-D695M-91 using an Instron universal testing machine (model-4502) at a cross-head speed of 1 mm/min. Cylindrical specimens with an aspect ratio of 2 were used for testing. At least five specimens were tested for each sample.

The kinetics of toluene absorption was determined for the nanocomposites at 25 °C. The diameter and thickness of the specimen were respectively 15 mm and about 1.0−1.5 mm, so that the thickness, $2L$, of the specimen is thin enough that molecular diffusion is considered to be one-dimensional. The samples were first weighed and conditioned at 25 °C in a desiccator containing toluene to ensure a relative humidity of 100% for toluene. The conditioning of the samples in a highly concentrated toluene atmosphere was preferred to the classical technique of immersion in toluene, because some samples can partially break down after immersion in toluene for a long time. The samples were then removed at specific intervals (t) and weighed (M_t) until an equilibrium weight gain value (M_∞) was obtained. The swelling rate of the samples was calculated by dividing the weight gain ($M_t - M_0$) by the initial weight (M_0). The mass of toluene absorbed ($M_t - M_0$) at time t can be expressed as follows[53]

$$\frac{M_t - M_0}{M_\infty} = 1 - \sum_{n=0}^{\infty} \frac{8}{(2n+1)^2\pi^2} \exp\left[\frac{-D(2n+1)^2\pi^2 t}{4L^2}\right] \quad (1)$$

where D is the diffusion coefficient. At short times, eq 1 can be written as

$$\frac{M_t - M_0}{M_\infty} = \frac{2}{L}\left(\frac{D}{\pi}\right)^{1/2} t^{1/2} \quad (2)$$

When the value of $(M_t - M_0)/M_\infty$ is less than 0.5, the error in using eq

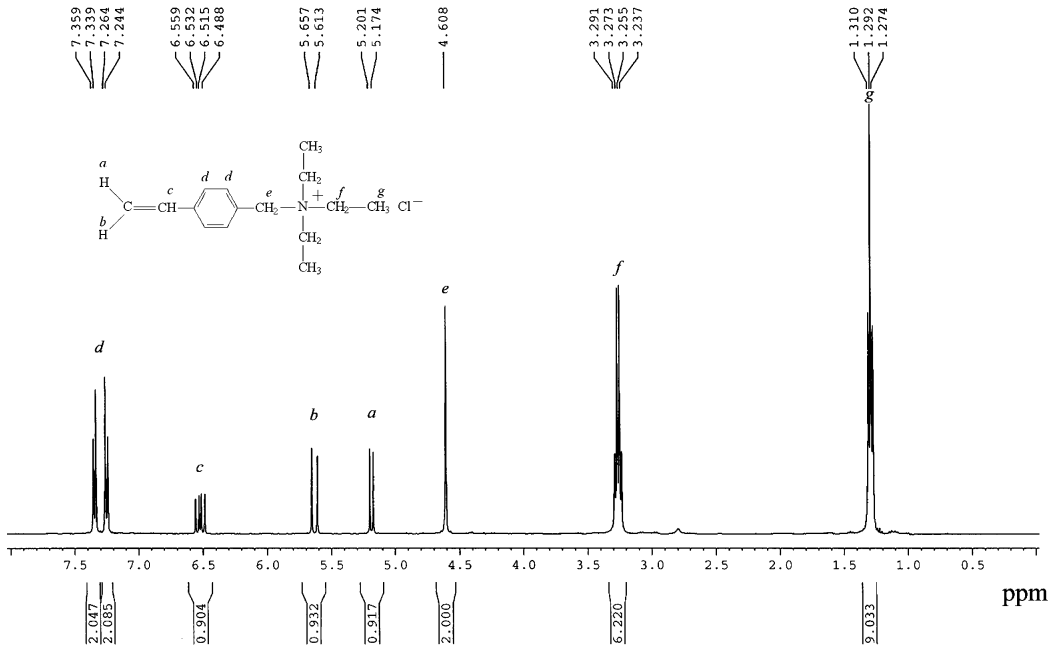

Figure 1. ^{1}H NMR spectrum of (4-vinylbenzyl)triethylammonium chloride (VTAC).

2, instead of eq 1, to determine the diffusion coefficient is on the order of 0.1%.[53] The diffusion coefficients of the samples were calculated from the slope of the first linear portion of these plots.

Results and Discussion

Functionalization of MMT. VTAC contains polymerizable vinyl aromatic groups that have good affinity with ST and DVB and can be polymerized into soybean oil-based polymer matrix, leading to improved interfacial compatibility between the organic matrix and the inorganic phases of the nanoparticles. Therefore, we synthesized the VTAC by reacting 4-vinylbenzyl chloride with triethylamine, and use the resulting cationic surfactant to modify the MMT for the preparation of some novel nanocomposites with improved physical properties. The characteristic ^{1}H NMR spectrum of VTAC in $CDCl_3$ and the peak assignments shown in Figure 1 indicate that VTAC was successfully synthesized. VTAC is readily soluble in polar solvents, such as water, alcohol, acetone, etc. After modification of MMT, about 70% sodium ions in MMT calculated from the TGA data have been exchanged by VTAC. The resulting VMMT exhibits a hydrophobic nature and is easily dispersed in an organic mixture of oil, ST, and DVB. The typical WAXD patterns of MMT and VMMT are shown in Figure 2. MMT exhibits a broad peak at $2\theta = 7.6°$, corresponding to a diffraction peak of the (001) plane of layered silicate. For VMMT, a very strong (001) diffraction peak is displayed at $2\theta = 5.9°$. On the basis of Bragg's law, $d = \lambda/2 \sin \theta$, where λ and θ are the X-ray wavelength (1.5418 Å) and diffraction angle, respectively, the (001) *d*-spacings of MMT and VMMT are calculated to be 1.15 and 1.51 nm, respectively. This means that the galleries of layered silicate in MMT are effectively intercalated by the VTAC surfactant, and thus the *d*-spacing is enlarged.[8,24]

Structure and Morphology. Figure 3 shows the WAXD patterns of nanocomposites from CSOY50−ST25−DVB10−NFO10−BFE5 (a) and CLS50−ST25−DVB10−NFO10−BFE5 (b) containing differing VMMT content. Because the neat polymers CSOY50−ST25−DVB10−NFO10−BFE5 and CLS50−ST25−DVB10−NFO10−BFE5 do not have any diffraction peak in the 2θ range from 2 to 10° (not shown), diffraction

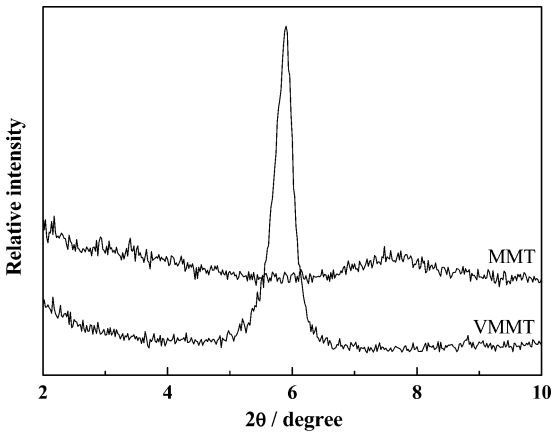

Figure 2. WAXD patterns for MMT and VMMT.

peaks appearing in the WAXD patterns of the nanocomposites are fully contributed by the diffraction peaks of VMMT. The CSOY- and CLS-based nanocomposites with the same VMMT loading display similar diffraction patterns. For nanocomposites with 1 wt % VMMT, the (001) diffraction peak disappears at 2θ from 2 to 10°. This is possibly due to that the organophilic treatment by VTAC reduces the attractive forces between the silicate layers and, therefore, facilitates the penetration of the CSOY, CLS, ST, and DVB into the inter-gallery space of VMMT, resulting in the exfoliated layered silicates after polymerization.[54] However, the WAXD results alone are insufficient to determine the extent of the exfoliated clay in the nanocomposites, because the WAXD sometimes may not give strong signal. For example, stacks of about 2−20 layers of clay are well dispersed in the polymer matrix. In this case, the diffraction peak of the ordered structure disappears, despite the fact that stacked layers still exist.[55] Therefore, the results from WAXD have always been further verified by TEM observation, which provides direct visualization of the morphology and spatial distribution of the clay platelets.[5] With an increase in the VMMT concentration from 2 to 5 wt %, the small diffraction peak at $2\theta = 5.8-5.6$, which shifts to a lower angle and decrease significantly in intensity as compared with that of VMMT, is observed for the samples. This implies that the

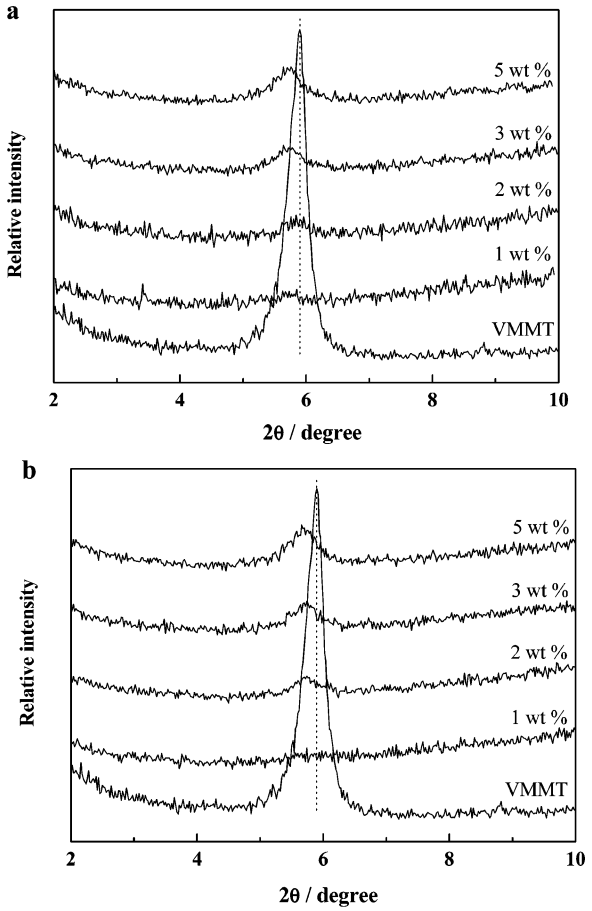

Figure 3. WAXD patterns for VMMT and nanocomposites from CSOY50−ST25−DVB10−NFO10−BFE5 (a) and CLS50−ST25−DVB10−NFO10−BFE5 (b) with different VMMT loadings.

soybean oil-based polymers are intercalated into the interlayers of the silicates.[5]

Figure 4 shows TEM images of the nanocomposites from CSOY50−ST25−DVB10−NFO10−BFE5 with 1, 2, and 5 wt % VMMT. The nanocomposites have intercalated structures, in which the stacked layers exist. However, some individual silicate layers can be observed from Figure 4, parts a and b. Thus, the morphology of the nanocomposites with 1 and 2 wt % VMMT can be considered as a heterogeneous system comprised of intercalated and partially exfoliated structures.[5] For the sample reinforced with 5 wt % VMMT, the swollen VMMT maintains a fairly ordered structure, resulting in an intercalated structure. This can be explained by the fact that, during the bulk polymerization, the high viscosity of the hybrid mixture, due to addition of the VMMT, makes it difficult for the monomer molecules to diffuse into the clay galleries effectively, leading to the penetration of only a few polymer molecules into the layered silicates.[4]

Both X-ray diffraction and TEM show that the lower loading of VMMT favors intercalation of the polymer chains into the silicate layers during polymerization, resulting in a heterogeneous structure consisting of intercalation and partially exfoliation. At higher VMMT loadings, the polymer chains intercalate only into the silicate layers without any major disruption of the ordered structure of VMMT, and thus lead to an intercalated structure.

Thermophysical Properties. The dynamic storage modulus (E') and loss factor (tan δ) for the nanocomposites from CSOY50−ST25−DVB10−NFO10−BFE5 with different VMMT loadings are shown in Figure 5. The copolymer CSOY50−

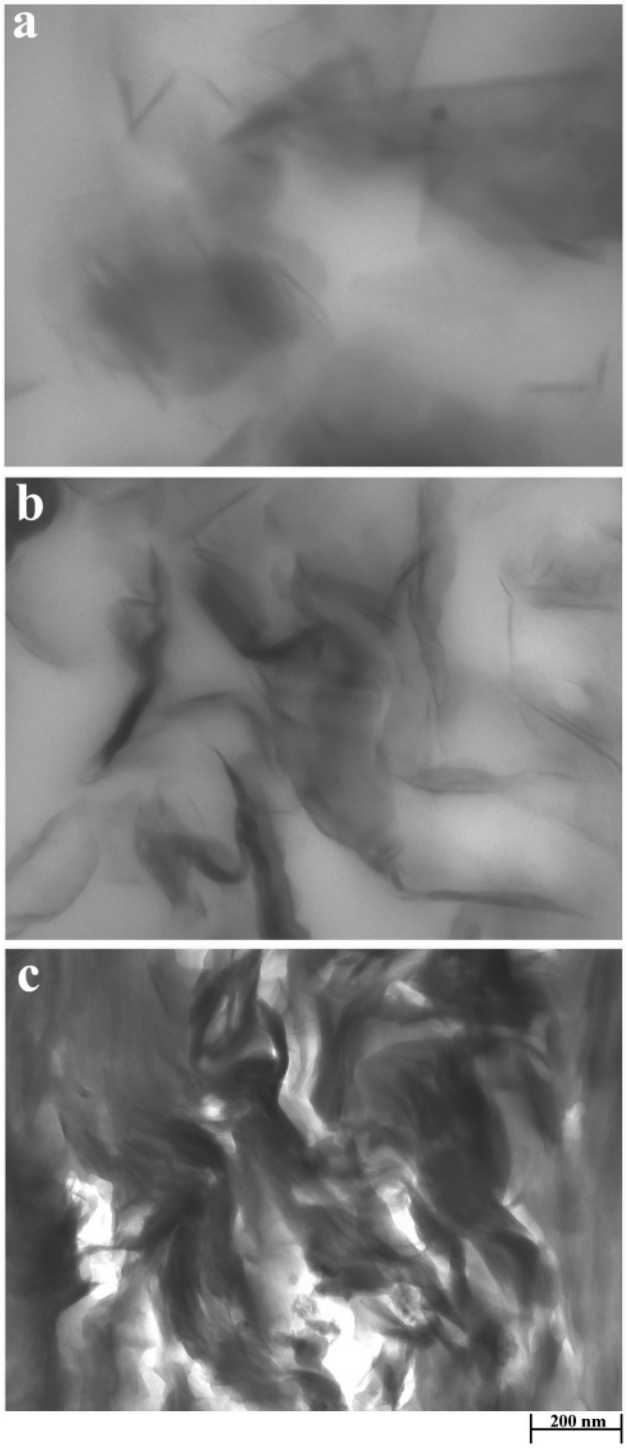

Figure 4. TEM images of nanocomposites from CSOY50−ST25−DVB10−NFO10−BFE5 with 1 (a), 2 (b), and 5 wt % (c) VMMT. Scale bar = 200 nm.

ST25−DVB10−NFO10−BFE5 exists in the glassy state at a very low temperature, and the modulus deceases slightly with increasing temperature. Then, a sharp decrease in the E' value is observed in the temperature range from −25 to +50 °C. This corresponds to the primary relaxation process (α) of the soybean oil-based polymers, where tan δ goes through a maximum. Then, the modulus reaches a plateau around 6 MPa, corresponding to the rubbery state of the polymer. The rubbery modulus remains constant until about 170 °C, the temperature at which the polymer begins to degrade thermally. Similar to the neat polymer, all nanocomposites exhibit a dramatic drop in E' value

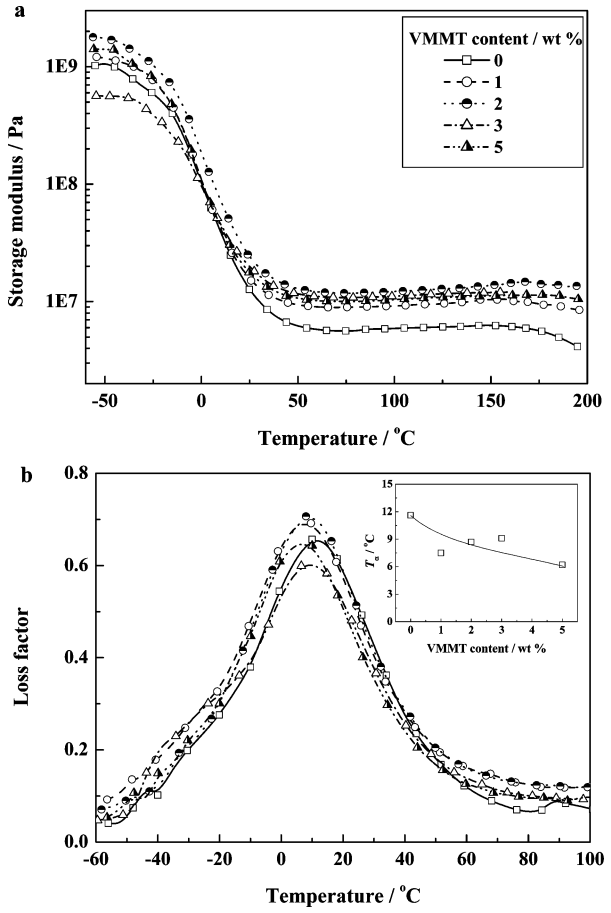

Figure 5. DMA behavior of nanocomposites from CSOY50−ST25−DVB10−NFO10−BFE5 with different VMMT loadings.

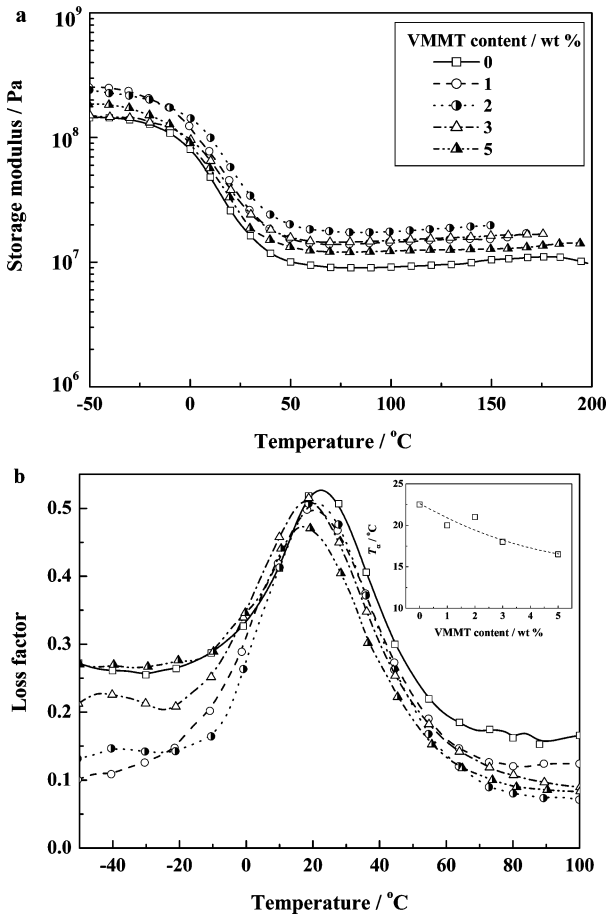

Figure 6. DMA behavior of nanocomposites from CLS50−ST25−DVB10−NFO10−BFE5 with different VMMT loadings.

in the temperature range from −50 to +50 °C, followed by a rubbery plateau. The rubbery modulus of the nanocomposites is significantly improved by incorporating VMMT. For instance, the rubbery modulus of the CSOY-based nanocomposites at 100 °C containing 1, 2, 3, and 5 wt % VMMT is about 1.6, 2.1, 1.9, and 1.7 times higher, respectively, than that for the CSOY-based polymer itself. This modulus improvement is retained up to 200 °C or even higher, indicating reinforced rigidity and higher thermal stability due to the fact that the nanoscale clay platelets restrict the matrix segmental motions at VMMT-polymer interface.[5] The tan $\delta - T$ curve of the polymer CSOY50−ST25−DVB10−NFO10−BFE5 shows one relaxation process, which involves energy dissipation and cooperative chain motions.[56] When increasing the VMMT loading from 0 to 5 wt % in the matrix, the relaxation temperature (T_α) of the samples, defined as the peak position of tan δ, shifts from 11.6 to 6.2 °C (Figure 5b, top right). Similar results have been reported in organoclay-reinforced polystyrene,[24] vinylester resin,[29] epoxy[5] and acrylated epoxidized soybean oil-styrene copolymers.[49] The reduction of T_α in this work may be attributed to the high viscosity of the hybrid reactant that affects diffusion of the initiator and chain propagation during polymerization, leading to a loose network structure for the polymer matrix. A decrease in the molecular weight of the polystyrene matrix, due to the high viscosity of the medium, has also been found in an in situ polymerized nanocomposite from styrene and an organoclay.[24] Another possibility is that the DVB and ST can more easily penetrate into the clay layers than the triglyceride-based monomers, because of their smaller size. The aromatic nature of ST and DVB imparts rigidity to the resulting CSOY-based network, and the loss of ST and DVB from the clay layers decreases the rigidity of the polymer matrix, which results in an overall reduction in T_α.[48] It is noteworthy that all nanocomposites from CSOY50−ST25−DVB10−NFO10−BFE5 exhibit a loss peak that is higher than 0.3 over a wide temperature range ($\Delta T = 55-61$ °C). Thus, these nanocomposites have very good damping properties and potential applications where the reduction of both unwanted noise and resonance vibrations is important.[56]

Figure 6 shows the dynamic storage modulus (E') and loss factor (tan δ) of the nanocomposites from CLS50−ST25−DVB10−NFO10−BFE5 with different VMMT loadings. As expected, the polymer CLS50−ST25−DVB10−NFO10−BFE5 shows a higher rubbery plateau modulus (10 MPa) than the polymer CSOY50−ST25−DVB10−NFO10−BFE5, due to the higher cross-link density of the CLS-based polymer. Similar to the nanocomposites from CSOY50−ST25−DVB10−NFO10−BFE5, the nanocomposites from CLS50−ST25−DVB10−NFO10−BFE5 show a significant improvement in storage modulus when compared to the pure polymer. The plateau modulus of the nanocomposites at 100 °C increases by 1.6, 1.9, 1.6, and 1.4 times when the VMMT content is 1, 2, 3, and 5 wt %, respectively. Meanwhile, the T_α of the nanocomposites decreases from 22.5 to 16.5 °C when increasing the VMMT loading in the matrix from 0 to 5 wt %. Unlike the CSOY-based nanocomposites, the CLS-based nanocomposites show a decrease in the intensity of the tan δ peak when compared with the polymer CLS50−ST25−DVB10−NFO10−BFE5. As shown in our previous work,[39] CLS has a higher degree of unsaturation than CSOY, which makes it more reactive toward ST and DVB than the CSOY, leading to higher incorporation of the oil and a more highly cross-linked copolymer. The C═C bonds on the

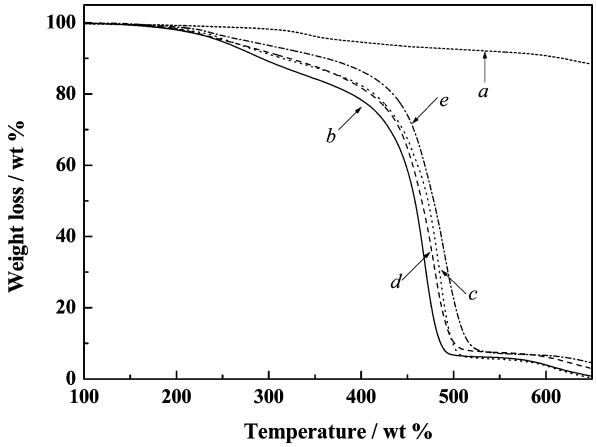

Figure 7. TGA curves of VMMT (a), CSOY50−ST25−DVB10−NFO10−BFE5 (b), CLS50−ST25−DVB10−NFO10−BFE5 (c), and nanocomposites from CSOY (d) and CLS (e) with 2 wt % VMMT.

VMMT surface have a similar reactivity with that of ST and DVB, so VMMT can be more homogeneously polymerized into the CLS-based matrix than the CSOY-based matrix. The relatively homogeneous nanostructure of the resulting CLS-based materials restricts the polymer segmental motions at the VMMT−polymer matrix interface and, therefore, results in a decreased intensity of the tan δ peak.[56]

Montmorillonite nanolayers consist of tetrahedral-octahedral silicate sheets with well-ordered spatial architecture. When exfoliated within a polymeric matrix, silicate nanolayers are expected to retard thermal degradation due to the lower heat diffusion into the polymer matrix. As a consequence, exfoliated nanolayers are expected to enhance the thermal stability of the nanocomposites by acting as a superior insulator and mass transport barrier to the volatile products generated during decomposition.[1,14] The TGA curves of VMMT, the polymers of CSOY50−ST25−DVB10−NFO10−BFE5 and CLS50−ST25−DVB10−NFO10−BFE5, and the corresponding nanocomposites with 2 wt % VMMT are shown in Figure 7, and the thermal data for all nanocomposites are summarized in Table 1. A weight loss of about 12 wt % is found for VMMT at about 600 °C, corresponding to the degradation of the vinylbenzyltriethylammonium. The CSOY-based polymer shows a three-stage weight loss. The initial loss, beginning at around 200 °C, is attributed to evaporation and decomposition of the unreacted oil and other soluble components in the bulk materials.[39] The second loss at around 400−500 °C is believed to be caused by pyrolysis of the cross-linked polymer networks. The final loss at around 600 °C is indicative of complete decomposition of the smaller fragments and oxidation of the carbon residue. As expected, the polymer CLS50−ST25−DVB10−NFO10−BFE5 shows a higher thermal stability than the polymer CSOY50−ST25−DVB10−NFO10−BFE5, since the CLS-based polymer is relatively highly cross-linked.[39] The TGA curves for the CSOY- and CLS-based nanocomposites with 2 wt % VMMT shift to a higher temperature when compared with those of the corresponding polymers, indicating the higher thermal stabilities of the resulting nanocomposites. The interesting parameters from the TGA curves for the nanocomposites have been taken from the onset of degradation, which is usually taken as the temperature at which 10% degradation occurs, T_{10}, the midpoint temperature of the degradation (T_{50}), the maximum degradation temperature (T_{max}), and the nonvolatile residue, which remains at 650 °C, denoted as char. The thermal degradation behavior of the nanocomposites is largely influenced by the VMMT loading. The T_{10} values of the CSOY-based nanocomposites increase from 293 to 335 °C with an increase in the VMMT content from 0 to 5 wt %. In the meanwhile, increases of 11 °C in T_{50} and 7 °C in T_{max} are observed for the sample with 2 wt % VMMT. For the CLS-based nanocomposites, the greatest improvements of 48, 5, and 7 °C are found in T_{10}, T_{50}, and T_{max} for the sample with 2 wt % of VMMT. These results indicate that VMMT plays an important role in enhancing the thermal stability of the soybean oil-based nanocomposites. The improvement may be attributed to the interfacial interactions between organic and inorganic phases. Similar results have also been reported for the nanocomposites of PP-EP/EVA/organo-clay[14] and polystyrene/clay.[15] Nanocomposites with 5 wt % VMMT exhibit no obvious improvement in T_{50} and T_{max} values when compared to the pure polymers. As mentioned earlier, the higher the concentration of VMMT, the higher the viscosity of the reactants and hence the lower the cross-link density of the polymer matrix, which makes it easier for random scission decomposition of the polymer main chains. The char formed at 650 °C increases slightly with increasing VMMT content in the matrix and equals the amount of VMMT that has been added. The variations are within experimental error.

Mechanical Properties. Compressive mechanical tests have been performed to quantify the overall effect of the VMMT on the performance of the soybean oil-based nanocomposites. The modulus, the strength, and the strain at failure of the samples from CSOY50−ST25−DVB10−NFO10−BFE5 and CLS50−ST25−DVB10−NFO10−BFE5 as a function of the VMMT content are shown in Figure 8. As expected, the polymer from CLS exhibits the higher mechanical properties, including modulus, strength and strain at failure, than the CSOY-based polymer, owing to its higher unsaturation and higher reactivity toward ST and DVB. For the nanocomposites, it is worth noting that the modulus, strength and strain at failure for both the CSOY- and CLS-based nanocomposites are simultaneously optimal at a low amount of VMMT. When the VMMT loading

Table 1. TGA Data for Soybean Oil-Based Polymers and the Resulting Nanocomposites

	nanocomposites					
no.	matrix	VMMT/wt %	T_{10}/°C	T_{50}/°C	T_{max}/°C	char % at 650 °C
1	CSOY50−ST25−DVB10−NFO10−BFE5	0	293	469	459	0.9
2		1	293	467	454	1.2
3		2	322	480	466	3.1
4		3	325	476	462	3.7
5		5	335	470	461	4.7
6	CLS50−ST25−DVB10−NFO10−BFE5	0	317	481	471	0.4
7		1	342	483	469	2.0
8		2	365	486	478	4.4
9		3	360	482	476	4.0
10		5	358	480	472	4.3

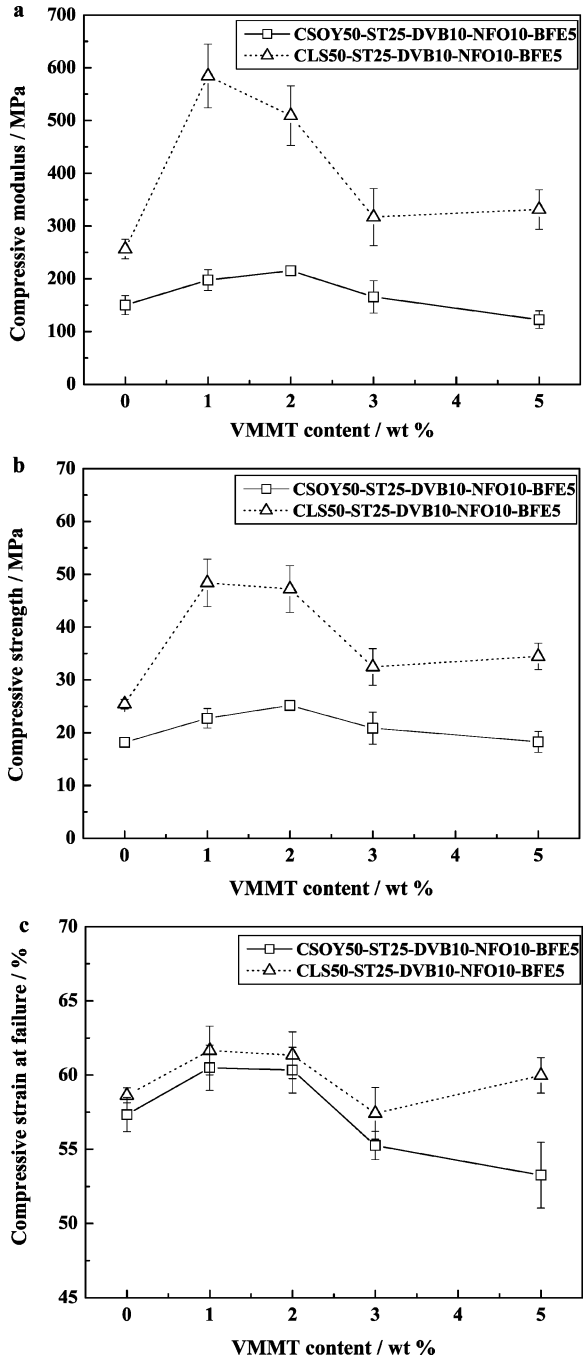

Figure 8. Compressive modulus (a), compressive ultimate strength (b) and compressive strain at failure (c) for the nanocomposites from CSOY50−ST25−DVB10−NFO10−BFE5 and CLS50−ST25−DVB10−NFO10−BFE5 as a function of VMMT loading.

is in the range of 1−2 wt %, the modulus is found to increase by about 31−43% and 100−128% for the resulting nanocomposites from CSOY and CLS, respectively. In the meanwhile, the compressive strength of the CSOY- and CLS-based nanocomposites also increases from 17 to 23 MPa and from 25 to 48 MPa, respectively. These results indicate an improvement in elasticity of the nanocomposites, which can be due to the strong interfacial interaction between the soybean oil-based polymer and the silicate platelets and to the presence of immobilized or partially immobilized polymer phases.[4] When the VMMT loading is further increased, the modulus does not increase as expected. This can be attributed to defects in polymer networks as described earlier, and by the intercalation of VMMT that decreases the polymer-layered silicate interfacial bonding

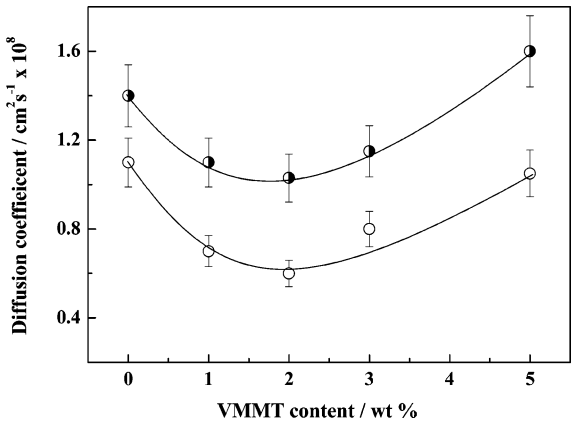

Figure 9. Toluene diffusion coefficients for CSOY- (◑) and CLS-based nanocomposites (○) as a function of VMMT loading.

and prevents the monomers from penetrating into the galleries of the VMMT. From Figure 8c, it is rather surprising and very interesting that the compressive strain at failure is also increased by about 7% in the presence of 1−2 wt % VMMT in the matrix from CSOY and CLS. As is well-known, an increase in the material modulus and strength results usually in a decrease in the strain for most polymers or polymer composites. However, by incorporating a small amount of VMMT in the soybean oil based resin, the modulus, strength, and strain at failure of the resulting nanocomposites increase simultaneously. When increasing the VMMT content from 3 to 5 wt %, a decrease in the strain at failure is observed, because the clay particles are rigid fillers and make the resulting nanocomposite more brittle at high VMMT content.[4]

It is interesting to note that the reinforcement efficiency of VMMT for the polymer CLS50−ST25−DVB10−NFO10−BFE5 is much higher than for the polymer CSOY50−ST25−DVB10−NFO10−BFE5, especially with a low VMMT loading of less than 2 wt %. As mentioned earlier, the higher unsaturation and higher reactivity of CLS results in more homogeneous polymerization of the VMMT in the polymer matrix of CLS50−ST25−DVB10−NFO10−BFE5, and thus leads to a more homogeneous nanostructure, resulting in much improved mechanical properties for the resulting nanocomposites.

Organic Vapor Diffusion Behavior. Diffusion behavior of a solvent into a cross-linked polymer is complex and remains a challenge to understand. Diffusion depends strongly on the temperature, the solvent molecular weight, the cross-linking density of the polymer, the polymer−solvent interactions and other factors. A study of the process and the kinetics for diffusion of a solvent into the polymer can result in a better understanding of the polymer morphology and structure.[57] Figure 9 shows the toluene diffusion coefficients in the CSOY- and CLS-based nanocomposites as a function of the VMMT content. The diffusion coefficients of toluene in the CSOY- and CLS-based polymers are 1.1×10^{-8} and 1.4×10^{-8} cm^2 s^{-1}, respectively. However, the diffusion coefficients of the nanocomposites are decreased dramatically even at very low VMMT content and the minimum values of 0.6×10^{-8} and 1.0×10^{-8} cm^2 s^{-1} are found, respectively, for the nanocomposites from CSOY and CLS at 2 wt % VMMT loading. Taking into account the morphology of these soybean oil-based nanocomposites, some degree of exfoliation of the VMMT in the polymer matrix is a prerequisite to improving the barrier properties of the materials toward organic vapors. The exfoliated silicate platelets increase the diffusion distance by creating a tortuous path, which the diffusing molecules must traverse. Similar results have been reported for PCL/montmorillonite nanocomposites.[58] With an

increase of the VMMT loading from 3 to 5 wt % in the polymer matrix, the diffusion coefficients of the resulting nanocomposites increase. Furthermore, the nanocomposites with 5 wt % VMMT show similar or even higher diffusion coefficients when compared with the corresponding polymers with no VMMT. This can be explained by the fact that in the intercalated samples, the ordered structure of the VMMT does not constitute an effective barrier to diffusion of the toluene molecules, which can jump from one specific site to another.[58]

Conclusions

Novel biobased nanocomposites have been successfully prepared using a reactive VMMT as a reinforcing phase for the soybean oil-based polymers produced by the cationic polymerization of CSOY or CLS with ST and DVB. The results of WAXD combined with TEM show that the nanocomposites exhibit a heterogeneous structure consisting of intercalation and partial exfoliation of VMMT at a low VMMT loading of 1−2 wt % and an intercalated structure at higher VMMT loadings. The high viscosity of the hybrid reactant due to the addition of VMMT affects diffusion of the initiator and chain propagation during the polymerization and, therefore, leads to a loose network structure for the polymer matrix. The VMMT in the polymer matrix play an important role in enhancing the thermal stability, and the mechanical and barrier properties of the resulting nanocomposites. The thermal stability, dynamic storage modulus, compressive modulus, compressive strength, compressive strain at failure, and barrier performance have been simultaneously optimized for the CSOY- and CLS-based nanocomposites with VMMT loadings of 1−2 wt %, respectively, due to the strong interfacial interaction between the layered silicate platelets and the polymer matrix. For instance, significant increases in the CLS-based nanocomposites in compressive modulus from 256 to 584 MPa, compressive strength from 25 to 48 MPa, and compressive strain at failure from 58% to 62% are respectively found when the VMMT loading increases from 0 to 2 wt %. The intercalated nanocomposites with a VMMT loading of 3−5 wt % do not show much performance improvement as compared with the pure polymers. CLS exhibits higher unsaturation and higher reactivity toward ST and DVB than CSOY. So the reactive VMMT can be more homogeneously polymerized into the CLS-based polymer matrix and thus result in a higher reinforcing efficiency of VMMT in the CLS-based polymer matrix than in the CSOY-based polymer matrix.

Acknowledgment. The authors gratefully acknowledge the Illinois−Missouri Biotechnology Alliance for financial support. We also thank Dr. Surya K. Mallapragada of the Department of Chemical Engineering and Dr. Jay-Lin Jane of the Department of Food Science and Human Nutrition at Iowa State University for the use of their facilities.

References and Notes

(1) Sinha Ray, S.; Okamoto, M. *Prog. Polym. Sci.* **2003**, *28*, 1539−1641.
(2) Giannelis, E. P. *Adv. Mater.* **1996**, *8*, 29−35.
(3) Weon, J.-I.; Sue, H.-J. *Polymer* **2005**, *46*, 6325−6334.
(4) Basara, C.; Yilmazer, U.; Bayram, G. *J. Appl. Polym. Sci.* **2005**, *98*, 1081−1086.
(5) Liu, T.; Tjiu, W. C.; Tong, Y.; He, C.; Goh, S. S.; Chung, T. S. *J. Appl. Polym. Sci.* **2004**, *94*, 1236−1244.
(6) Lee, A.; Lichtenhan, J. D. *J. Appl. Polym. Sci.* **1999**, *73*, 1993−2001.
(7) Park, H.-M.; Liang, X.; Mohanty, A. K.; Misra, M.; Drzal, L. T. *Macromolecules* **2004**, *37*, 9076−9082.
(8) Dai, X.; Xu, J.; Guo, X.; Lu, Y.; Shen, D.; Zhao, N.; Luo, X.; Zhang, X. *Macromolecules* **2004**, 37, 5615−5623.
(9) Chen, G.-X.; Yoon, J.-S. *Polym. Degrad. Stab.* **2005**, *88*, 206−212.
(10) Hasegawa, N.; Okamoto, H.; Kato, M.; Usuki, A.; Sato, N. *Polymer* **2003**, *44*, 2933−2937.
(11) Xu, R.; Manias, E.; Snyder, A. J.; Runt, J. *Macromolecules* **2001**, *34*, 337−339.
(12) Bharadwaj, R. K. *Macromolecules* **2001**, *34*, 9189−9192.
(13) Qin, H.; Zhang, S.; Zhao, C.; Hu, G.; Yang, M. *Polymer* **2005**, *46*, 8386-8395.
(14) Valera-Zaragoza, M.; Ramírez-Vargas, E.; Medellín-Rodríguez, F. J.; Huerta-Martínez, B. M. *Polym. Degrad. Stab.* **2006**, *91*, 1319−1325.
(15) Su, S.; Jiang, D. D.; Wilkie, C. A. *Polym. Degrad. Stab.* **2004**, *83*, 333−346.
(16) Chen, J. S.; Poliks, M. D.; Ober, C. K.; Zhang, Y.; Wiesner, U.; Giannelis, E. P. *Polymer* **2002**, *43*, 4895−904.
(17) Dubois, P.; Alexandre, M. *Adv. Eng. Mater.* **2006**, *8*, 147−154.
(18) Biswas, M.; Ray, S. S. *Adv. Polym. Sci.* **2001**, *155*, 167−221.
(19) Ren, T.; Yang, J.; Huang, Y.; Ren, J.; Liu, Y. *Polym. Compos.* **2006**, *27*, 55−64.
(20) Park, J. H.; Jana, S. C. *Macromolecules* **2003**, *36*, 2758−2768.
(21) Mitchell, C. A.; Krishnamoorti, R. *Polymer* **2005**, *46*, 8796−8804.
(22) Lan, T.; Pinnavaia, T. J. *Chem. Mater.* **1994**, *6*, 573−575.
(23) Lan, T.; Kaviratna. P. D.; Pinnavaia. T. J. *Chem. Mater.* **1995**, *7*, 2144−2150.
(24) Fu, X.; Qutubuddin, S. *Polymer* **2001**, *42*, 807−813.
(25) Dennis, H. R.; Hunter, D. L.; Chang, D.; Kim, S.; White, J. L.; Cho, J. W.; Paul, D. R. *Polymer* **2001**, *42*, 9513−9522.
(26) Maiti, P.; Nam, P. H.; Okamoto, M.; Hasegawa, N.; Usuki, A. *Macromolecules* **2002**, *35*, 2042−2049.
(27) Hasegawa, N.; Okamoto, H.; Kato, M.; Usuki, A. *J. Appl. Polym. Sci.* **2000**, *78*, 1918−1922.
(28) Tien, Y. I.; Wei, K. H. *Macromolecules* **2001**, *34*, 9045−9052.
(29) Someya, Y.; Shibata, M. *Polym. Eng. Sci.* **2004**, *44*, 2041−2046.
(30) Zhang, J.; Jiang, L.; Zhu, L.; Jane, J.-L.; Mungara, P. *Biomacromolecules* **2006**, *7*, 1551−1561.
(31) Nayak, P. L. *J. Macromol. Sci.: Rev. Macromol. Chem. Phys.* **2000**, *40*, 1−21.
(32) Khot, S. N.; LaScala, J. J.; Can, E.; Morye, S. S.; Williams, G. I.; Palmese, G. R.; Husefoglu, S. H.; Wool, R. P. *J. Appl. Polym. Sci.* **2001**, *82*, 703−723.
(33) Mosiewicki, M.; Aranguren, M. I.; Borrajo, J. *J. Appl. Polym. Sci.* **2005**, *97*, 825−836.
(34) Miyagawa, H.; Misra, M.; Drzal, L. T.; Mohanty, A. K. *Polym. Eng. Sci.* **2005**, *45*, 487−495.
(35) Petrović, Z. S.; Guo, A.; Zhang, W. *J. Polym. Sci., Part A: Polym. Chem.* **2000**, *38*, 4062−4069.
(36) Lu, Y. S.; Tighzert, L.; Dole, P.; Erre, D. *Polymer* **2005**, *46*, 9863−9870.
(37) Lu, Y. S.; Tighzert, L.; Berzin, F.; Rondot, S. *Carbohydr. Polym.* **2005**, *61*, 174−182.
(38) Li, F.; Hanson, M. V.; Larock, R. C. *Polymer* **2002**, *42*, 1567−1579.
(39) Li, F.; Larock, R. C. *J. Appl. Polym. Sci.* **2001**, *80*, 658−670.
(40) Li, F.; Larock, R. C. *J. Polym. Sci., Part B: Polym. Phys.* **2001**, *39*, 60−77.
(41) Andjelkovic, D. D.; Larock, R. C. *Biomacromolecules* **2006**, *7*, 927−936.
(42) Kundu, P. P.; Larock, R. C. *Biomacromolecules* **2005**, *6*, 797−806.
(43) Li, F.; Larock, R. C. *Biomacromolecules* **2003**, 4, 1018−1025.
(44) Li, F.; Larock, R. C. *J. Appl. Polym. Sci.* **2000**, *78*, 1044−1056.
(45) Li, F.; Larock, R. C. *J. Appl. Polym. Sci.* **2003**, *90*, 1830−1838.
(46) Marks, D. W.; Li, F.; Pacha, C. M.; Larock, R. C. *J. Appl. Polym. Sci.* **2001**, *81*, 2001−2012.
(47) Li, F.; Larock, R. C. In *Natural Fibers, Biopolymers, and Biocomposites*; Mohanty, A. K., Misra, M., Drzal, L. T., Eds.; CRC Press: Boca Raton, FL, 2005.
(48) Lu, J.; Hong, C. K.; Wool, R. P. *J. Polym. Sci., Part B: Polym. Phys.* **2004**, *42*, 1441−1450.
(49) Uyama, H.; Kuwabara, M.; Tsujimoto, T.; Nakano, M.; Usuki, A.; Kobayashi, S. *Macromol. Biosci.* **2004**, *4*, 354−360.
(50) Uyama, H.; Kuwabara, M.; Tsujimoto, T.; Nakano, M.; Usuki, A.; Kobayashi, S. *Chem. Mater.* **2003**, *15*, 2492−2494.
(51) Miyagawa, H.; Misra, M.; Drzal, L. T.; Mohanty, A. K. *Polymer* **2005**, *46*, 445−453.
(52) Larock, R. C.; Dong, X. Y.; Chung, S.; Reddy, K.; Ehlers, L. E. *J. Am. Oil Chem. Soc.* **2001**, *78*, 447−453.
(53) Vergnaud, J. M. *Liquid Transport Process in Polymeric Materials: Modeling and Industrial Applications*; Prentice Hall: Englewood Cliffs, NJ, 1991.

(54) Priya, L.; Jog, J. P. *J. Polym. Sci., Part B: Polym. Phys.* **2003**, *41*, 31−38.
(55) Yoonessi, M.; Toghiani, H.; Kingery, W. L.; Pittman, C. U., Jr. *Macromolecules* **2004**, *37*, 2511−2518.
(56) Uthirakumar, P.; Hahn, Y. B.; Nahm, K. S.; Lee, Y.-S. *Eur. Polym. J.* **2005**, *41*, 1582−1588.
(57) Gopalan Nair, K.; Dufresne, A. *Biomacromolecules* **2003**, *4*, 657−665.
(58) Gorrasi, G.; Tortora, M.; Vittoria, V.; Pollet, E.; Lepoittevin, B.; Alexandre, M.; Dubois, P. *Polymer* **2003**, *44*, 2271−2279.

BM060458E